Chemotherapy: Open Access
ISSN: 2167-7700
OPEN ACCESS Freely available online
Research Article

Cancer Cells in all EMT States Lack Rigidity Sensing Depletion of Different Tumor Suppressors Causes Loss of Rigidity Sensing in Cancer Cells

Chloe Simpson[1,2], Vignesh Sundararajan[2], Tuan Zea Tan[2], Ruby Huang[2,3], Michael Sheetz[1,4,5*]

[1]Department of Mechanobiology, Mechanobiology Institute, National University of Singapore, Queenstown, Singapore;[2]Department of Cancer Science Institute of Singapore, National University of Singapore, Queenstown Singapore;[3]Department of Medicine and Graduate, Institute of Oncology, College of Medicine, National Taiwan University, Taipei, Taiwan;[4]Department of Biochemistry and Molecular Biology, University of Texas Medical Branch, Galveston, TX, USA;[5]Department of Biological Sciences, Columbia University, New York, NY, USA

ABSTRACT

Cancer cells have many different behaviors from epithelial to mesenchyme forms. We report here that 36 distinct tumor cell lines regardless of EMT form or other features lack the ability to sense rigidity and will grow on soft surfaces. In the majority of lines, cells were missing at least one protein needed for rigidity sensing (primarily tropomyosin 2.1 (Tpm2.1) but also PTPN12, FilaminA (FLNA), and myosin IIA) while all had high levels of Tpm3. In the few cases where the major rigidity sensing components were present, those tumor cells were not able to sense rigidity. Thus, we suggest that tumor cells can lose the ability to sense rigidity by many different means and that the loss of rigidity sensing is sufficient to cause the transformed phenotype that enables targeted treatments.

Keywords: Cancer cells; Tumor suppressors; Tumor; Treatments

INTRODUCTION

For many years, it has been evident that the frequency of cancerous tumors correlates with the frequency of injury/inflammation events [1]. In both regeneration and cancer, the blocks to adult cell growth are removed; but in normal regeneration, the blocks are restored [2]. In the case of tumorigenic growth, the blocks to growth remain off and cells have the ability to grow in a variety of environments, even on soft matrices, often with the aid of activating hormones [3]. Early studies of tumor cells showed that they all were able to grow on soft surfaces i.e., were transformed; whereas normal cells required rigid surfaces to grow [4,5]. Recent findings support the hypothesis that the removal of the block to growth in cancers and the ability to grow on soft surfaces may be linked. In particular, the transformed state can be induced by depleting rigidity sensors in normal cells from different tissues; and when rigidity sensing is restored to tumor cells; they require rigid surfaces for growth [6-9]. This has led to the hypothesis that all tumor cells are transformed through the loss of rigidity sensing.

In addition, tumor growth is linked to many different signalling pathways and there is a wide range of behaviors of tumor cells that has confounded general treatments of cancers. Often blocking one growth pathway such as caused by mutation of the EGF receptor with an EGFR inhibitor results in the shrinkage of the tumor but metastases often arise with other growth stimuli [10,11]. Thus, there is a general ability of tumor cells to grow and they can do so with many different stimuli. This can be understood if tumor cells lack the normal blocks to growth that are removed in wound healing. There are common markers for wound healing and tumor growth in many different systems including an increase in the levels of miR-21 that is highly expressed in brain [12], liver, skin and even axolotl limb regeneration [13-15]. Similarly, many tumor cells have increased miR-21 levels that correlate with the severity of the cancer [16,17]. Since the loss of rigidity sensing enables normal cells to grow, we hypothesize that the loss of rigidity sensors plays a major role in tumor cells and that most if not all tumor cells will lack rigidity sensing.

Evidence from RNA sequencing has shown that the levels of many different mRNAs change upon the loss or restoration of rigidity sensing in cells from diverse tissues [18]. Thus, there appears to be a major state change upon transformation or the loss of rigidity sensing that results in general changes in cell behavior such as a

Correspondence to: Dr. Michael Sheetz, Department of Mechanobiology, Mechanobiology Institute, National University of Singapore, Queenstown, Singapore, E-mail: misheetz@utmb.edu

Received: : 01-Sep-2022, Manuscript No. CMT-22-18028; **Editor assigned:** 05- Sep-2022, Pre QC No. CMT-22-18028 (PQ); **Reviewed:** 19-Sep-2022, QC No. CMT-22-18028; **Revised:** 27-Sep-2022, Manuscript No. CMT-22-18028 (R); **Published:** 04-Oct-2022, DOI:10.35248/2167-7700.22.10.162.

Citation: Simpson C, Sundararajan V, Tan TZ, Huang R, Sheetz M (2022) Cancer Cells in all EMT States Lack Rigidity Sensing Depletion of Different Tumor Suppressors Causes Loss of Rigidity Sensing in Cancer Cells. Chemo Open Access. 10:162.

decrease in single cell rigidity [19-21], increased traction forces, and increased mechanical sensitivity [22-24]. If tumor cells have common properties regardless of the tissue and the exact cause of the tumor, then there may be treatments that would inhibit the growth of a wide diversity of tumors such as mechanical stress [25-27].

Alternatively, tumor cells often differ in many respects and one aspect that has been tied with the severity of the disease is the epithelial to mesenchyme transition that often comes with tumor progression in later stage disease. A bank of tumor cells that range from epithelial to mesenchyme has been characterized extensively in terms of morphology and markers for the epithelial and mesenchyme states [28-31]. We tested if they all have lost the ability to sense rigidity, which is consistent with our hypothesis that tumor cells should all lack the rigidity sensing whether or not they come from stage 1 or stage 4 tumors. Irrespective of the mutations involved and the phenotype, all the cell lines lacked rigidity sensors and grew on soft surfaces.

Figure 1 illustrates some of the key players linking mechanosensing and cancer. TPM2.1 for example has been reported as silenced and downregulated in breast, colorectal and urothelial bladder cancer [32-34]. In contrast TPM3 is most often overexpressed [35]. FLNA has a complex role in cancer, with both overexpression and loss of expression being associated with poor prognosis [36-40]. PTPN12 is a protein tyrosine phosphatase that binds to FLNA by a proline rich domain region, and is known to have interactions with various RTKs including INSR, INSRR, EGFR, as well as GRB2 and cSRC. In triple negative breast cancer restoration of PTPN12 has been shown to suppress EGFR, HER2, and PDGFRβ [41], where it acts as a tumour suppressor. In addition, decreased expression has previously been linked to increased motility in ovarian cancer [42]. Finally, myosin IIa has diverse roles in ovarian cancer [43-48], from increasing contractility in drug resistant tumours cells [49], clearing mesothelial cells during metastasis as well as being associated with cancer cell motility and migration (Figures 1) [50,51].

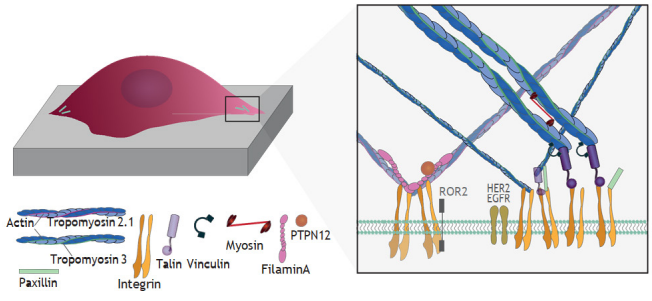

Figure 1: Analysis flow chart.

MATERIALS AND METHODS

Cell culture

BJ-5ta, IOSE523, OVCA433 and OVCA420 cells were cultured in DMEM with high glucose and supplemented with 10% FBS. OVCAR3 and IGROV1 cell lines were cultured in RPMI media supplemented with 10% FBS. Cells were incubated at 37°C, with 80% humidity and 5% $C0_2$.

Micropillar preparation and imaging

Micropillar production was done using precut silicone moulds. PDMS and crosslinker were mixed thoroughly in a ratio of 10:1 and degassed for 30 minutes at 10 MB. PDMS mixture was poured onto the mould degassed for 10 minutes at 10 MB. The mould was upturned onto a plasma cleaned glass bottomed plate, with a weight on top and further degassed for 10 minutes. The plate-mould-PDMS was then cured for 3 hours at 80°C. The PDMS was demoulded in isopropanol and washed 5x with PBS, or until no isopropanol remained. Before plating the PDMS micropillars were incubated with fibronectin at 37°C for 1 hour. PDMS was replaced with cell culture media and cells were plated, and incubated for 30 minutes before imaging. Cells were imaged in the DIC channel using EZ-live Olympus widefield microscope for 30 minutes at 1 frame per second.

TIFF movies of the cells spreading on micro pillars were corrected for imaging drift using the FIJI plugin stackreg with translation. Pillars were detected and deflections calculated using the Fiji plugin Pilartracker from MBI. Correlated pair deflections were assigned using the custom mat lab script.

PDMS surface preparation and imaging

To measure nematic order perameter of the actin fibres of cells, PDMS surfaces were produced using Sylgard 184 elastomer kit with varying ratios of elastomer to curing agent. For 2 MPa surfaces, the elastomer to curing agent ratio was 10:1, for 5 kPa surfaces the ratio was 75:1. Elastomer mixes were spin-coated onto plasma cleaned glass coverslips using a protocol of 200 RPM for 10 seconds and 1000 RPM for 1 minute. Slides were cured at 80°C for 3 hours. Slides were incubated with fibronectin for 1 hour at 37°C before cells were plated.

Fluorescence microscopy and analysis

Cells were trypsinised and plated onto both 2 MPa and 5 kPa slides and incubated for 6 hours at 37°C, at which point they were fixed in 4% Paraformaldehyde for 12 minutes at 37°C. Cells were permeablised with 0.5% Triton in PBS for 10 minutes at Room Temperature (RT) and blocked with 2% bovine serum albumin for 2 hours at RT. Primary antibody for paxillin (ab32084, abcam) was diluted in 2% BSA at a ratio of 1:1000 and incubated at RT for 2 hours. Secondary antibody Alexafluor-647 anti-rabbit at a dilution of 1:1000 and Phalloidin stain (A12379, Thermofisher) for f-actin at a dilution of 1:400 were mixed in 2% BSA added to slides and incubated for 1 hour at RT. The slides were washed 3x in PBS between each step. Cover slips were mounted onto glass slides using Dako mounting medium. Slides were imaged on W1 Live-SR spinning disk super resolution, and deconvolved to super resolution using the inbuilt LIVE-SR feature.

Western blot analysis

Whole cell protein lysates were used from the previously described ovarian cancer cell line library [52]. Cell lysates harvested in RIPA buffer were resolved through SDS-PAGE, followed by blotting on PVDF membranes. Immunoblots were subsequently incubated with appropriate primary antibodies: anti-Filamin-A (ab111620, Abcam); anti-Myosin-IIA (M8064, Sigma); anti-Tropomyosin 2 (T2780, Sigma); anti-Tropomyosin 3 (ab180813, Abcam), anti-β-Tubulin (ab7291, Abcam) diluted in 2% BSA in TBST. Secondary antibodies from Li-COR Biosciences were used: IRDye 800CW goat anti-mouse/rabbit (926-32210, 926-32211), IRDye 680LT goat anti-mouse/rabbit (926-68020, 926-68021). Immunoblots were scanned using the Odyssey Infrared Imaging System (Li-COR) and were converted to gray scale.

RESULTS

We selected a panel of 36 ovarian cancer cells lines of varied origin, one ovarian epithelial cell line and a human foreskin fibroblast cell line. The panel of ovarian cell lines was previously compiled to represent a full spectrum of epithelial to mesenchyme phenotypes [53], and originated from various ovarian cancer subtypes, diseases, and stages (Table 1). This panel included 12 cell lines of metastatic origin and 23 cell lines of primary tumour origin, with cells from ovarian serous adenocarcinoma, high grade ovarian serous adenocarcinoma, ovarian endometrioid carcinoma and ovarian cystadenocarcinoma. The panel includes several cell lines from epithelial, intermediate epithelial, intermediate mesenchyme and mesenchyme groups as categorised using methods previously described [54-56]. We assayed the protein levels of known mechanosensitive proteins TPM2.1, TPM3, FLNA, PTPN12 and Myosin IIa across the panel of cell lines by western blot and quantified these blots (Figures 2A and 2B). Intensity scores from western blots were standardized to a range of 0-1 to show relative expression of each protein, 1 being the highest expression observed across the panel of cell lines. We observed a striking phenotype whereby 18 of the 36 cell lines had no expression of TPM2.1 (Figure 2C), while all had TPM3 at levels equal to or greater than normal cell controls (Figure 2D). A further seven lines, OV90, OV56, TOV112D, HeyA8, Tyknu, SKOV3 and EF021 had no or very low expression of PTPN12 (Figure 2E). One cell line, EF021 had no FLNA (Figure 2F). One cell line, CH1 cells, had no Myosin IIa (Figure 2G). This demonstrates that loss of rigidity sensing proteins occurs in the majority of ovarian cancer cell lines. Co-occurring loss of TPM2.1 and PTPN12 was observed in four cell lines, TYKNu, OVCA420 and TOV112D, SKOV3, and the cell line with no FLNA, EF021 cells, also had low PTPN12. Thus, of the 36 cell lines, the majority had decreased levels of rigidity sensor proteins and all had high levels of Tpm3 that inhibits rigidity sensing [57]. Overall, no correlation was shown across the panel with epithelial to mesenchyme status and the expression of any of the assayed proteins across patient samples from CSIOVDB [58]; or in this panel of cell lines, indicating that the loss rigidity sensing is an early event in metastatic progression, occurring before EMT. A significant correlation was observed between expression of FLNA and MyosinIIA (Spearman r 0.4493, P=0.002) and between PTPN12 and TPM3 (Spearman r 0.414, p=0.012). We additionally assayed a few other known mechanosensitive proteins in 33 of the cell lines, TPM1, TPM2 (including TPM2.1 and other splice variants), DAPK, Piezo1 and mir21 RNA. All of the cell lines expressed these proteins and additional correlation was observed between DAPK and TPM1 expression (Spearman r 0.460, p=0.007).

We selected 3 tumor lines from the panel which retained all the proteins assayed (Figure 3A) and tested whether they had the ability to detect changes in substrate stiffness phenotypically. The three cell lines were IGROV1 which is an ovarian endometriod carcinoma cell line, OVCA433, and OVCA433, which are both ovarian serous adenocarcinoma cell lines, IOSE523 and OVCAR3 cell lines (Figure 3B). We also included two negative control lines, a human foreskin fibroblast cell line known to be capable of effective rigidity sensing BJ-3ta [59] and an ovarian epithelial cell line transformed using SV-40, IOSE523. We additionally included a positive control, a high grade ovarian serous carcinoma cell line which lacks TPM2.1, OVCAR3. As cells spread on the surface they tested the stiffness by contracting matrix adhesions [60,61]. This sarcomeric pinching was quantified by plating cells on PDMS micro pillars coated with fibronectin and analyzing pillar displacements over time [62]. As cells spread, the pillars were deflected in response to forces applied by the cell. Rigidity-sensing events were defined as contractile deflections of two pillars simultaneously by >30 nm for >20s such as those of pillar 1 and 2 whereas in many cases pillar deflections were not correlated (Figure 3C). The number of events per unit area per unit time was a measure of the cell's ability to sense rigidity. In this case, cells were plated on 0.8 μm pillars and imaged for 30 minutes, at a frame rate of 1 per second. An automated program determined the number of contractile events that fit the criteria for rigidity-sensing events from movies of the pillars covered by cells (see rigidity-sensing pillar deflections shown in green and non-correlated pillar deflections shown in red (Figure 3D).

Table 1: Panel of ovarian cancer cell lines, annotated with RRID, disease type, tumour stage, and EMT status.

Cell line	RRID	Disease	Tumour stage	EMT status
IOSE523	CVCL_E234	Ovarian epithelial (SV40 transformed)	N/a	Epithelial
CAOV3	CVCL_0201	High grade ovarian serous adenocarcinoma	Primary	Epithelial
OV90	CVCL_3768	Ovarian adenocarcinoma	Metastasis	Epithelial
OVCA420	CVCL_3935	Ovarian serous adenocarcinoma	Primary	Epithelial
OVCAR3	CVCL_0465	High grade ovarian serous adenocarcinoma	Metastasis	Epithelial
OVCAR8	CVCL_1629	High grade ovarian serous adenocarcinoma	Primary	Epithelial
PEO1	CVCL_2686	Ovarian cystadenocarcinoma	Metastasis	Epithelial
EFO21	CVCL_0029	Ovarian cystadenocarcinoma	Metastasis	Intermediate epithelial
FUOV1	CVCL_2047	High grade ovarian serous adenocarcinoma	Primary	Intermediate epithelial
IGROV1	CVCL_1304	Ovarian endometrioid adenocarcinoma	Primary	Intermediate epithelial
JHOS2	CVCL_4647	High grade ovarian serous adenocarcinoma	Primary	Intermediate epithelial
JHOS3	CVCL_4648	Ovarian serous adenocarcinoma	Primary	Intermediate epithelial
JHOS4	CVCL_4649	High grade ovarian serous adenocarcinoma	Primary	Intermediate epithelial

OAW28	CVCL_1614	High grade ovarian serous adenocarcinoma	Metastasis	Intermediate epithelial
OAW42	CVCL_1615	Ovarian cystadenocarcinoma	Metastasis	Intermediate epithelial
OV17R	CVCL_2672	Ovarian adenocarcinoma	Primary	Intermediate epithelial
OV56	CVCL_2673	Ovarian serous adenocarcinoma	Metastasis	Intermediate epithelial
OVCA429	CVCL_3936	Ovarian cystadenocarcinoma	Primary	Intermediate epithelial
OVCA432	CVCL_3769	Ovarian serous adenocarcinoma	Primary	Intermediate epithelial
OVCA433	CVCL_0475	Ovarian serous adenocarcinoma	Primary	Intermediate epithelial
OVCAR2	CVCL_3941	Ovarian carcinoma	Metastasis	Intermediate epithelial
OVCAR5	CVCL_1628	Ovarian serous adenocarcinoma	Primary	Intermediate epithelial
PEO4	CVCL_2690	Ovarian cystadenocarcinoma	Metastasis	Intermediate epithelial
UWB1.289	CVCL_B079	Ovarian carcinoma	Primary	Intermediate epithelial
A2780	CVCL_0134	Ovarian endometrioid adenocarcinoma	Primary	Intermediate mesenchymal
CH1	CVCL_4992	Ovarian mixed germ cell tumor	Metastasis	Intermediate mesenchymal
DOV13	CVCL_6774	Ovarian adenocarcinoma	Primary	Intermediate mesenchymal
HEY	CVCL_0297	High grade ovarian serous adenocarcinoma	Primary	Intermediate mesenchymal
HEYC2	CVCL_X009	High grade ovarian serous adenocarcinoma	Primary	Intermediate mesenchymal
OV7	CVCL_2675	Ovarian carcinoma	Primary	Intermediate mesenchymal
SKOV3	CVCL_0532	Ovarian serous cystadenocarcinoma	Metastasis	Intermediate mesenchymal
HEYA8	CVCL_8878	High grade ovarian serous adenocarcinoma	Primary	Mesenchymal
OVCAR10	CVCL_4377	Ovarian carcinoma	Primary	Mesenchymal
OVK18	CVCL_3770	Ovarian endometrioid adenocarcinoma	Metastasis	Mesenchymal
TOV112D	CVCL_3612	Ovarian endometrioid adenocarcinoma	Primary	Mesenchymal
TYKNu	CVCL_1776	High grade ovarian serous adenocarcinoma	Primary	Mesenchymal

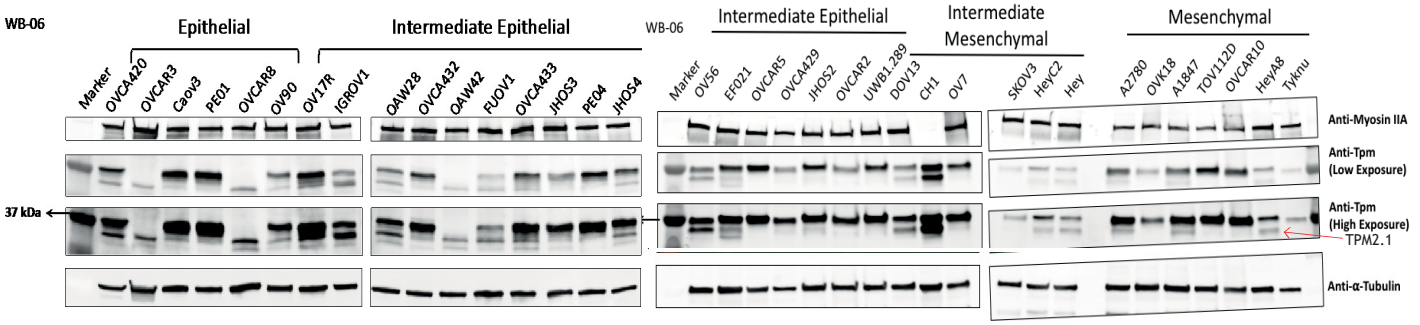

Figure 2A: Western blots of FilaminA and TPM3 in order of epithelial to mesnenchymal index.

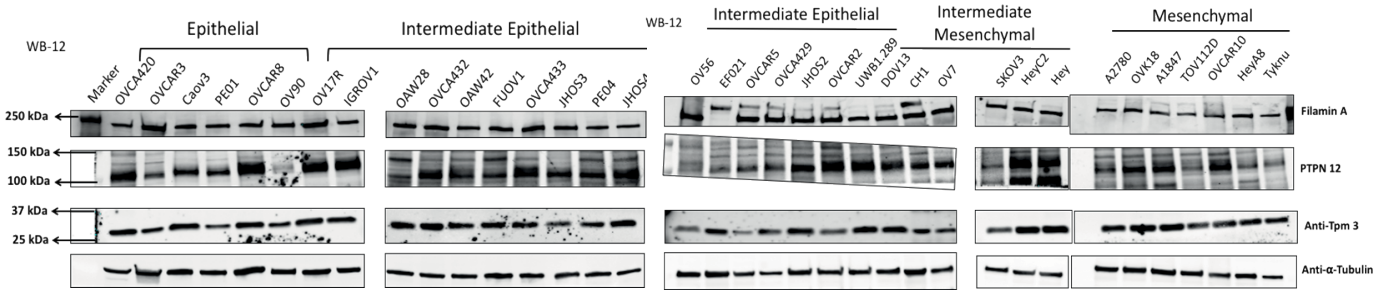

Figure 2B: Western blots of FilaminA and TPM3 in order of epithelial to mesnenchymal index.

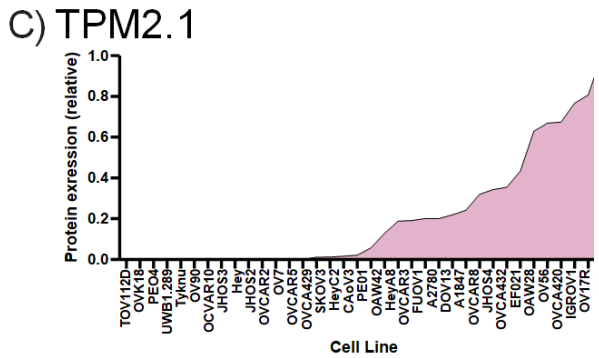

Figure 2C: Relative, normalised expression level of TPM2.1 in ovarian cancer cell lines ranked by ascending expression. Eighteen cell lines had no expression TPM2.1.

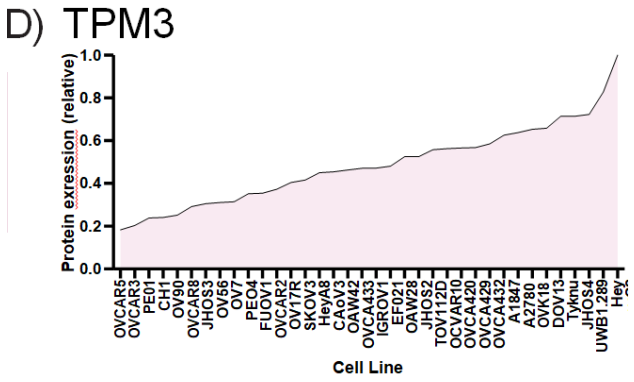

Figure 2D: Relative, normalised expression level of TPM3 in Ovarian cancer cell lines ranked by ascending expression. All cell lines expressed TPM3.

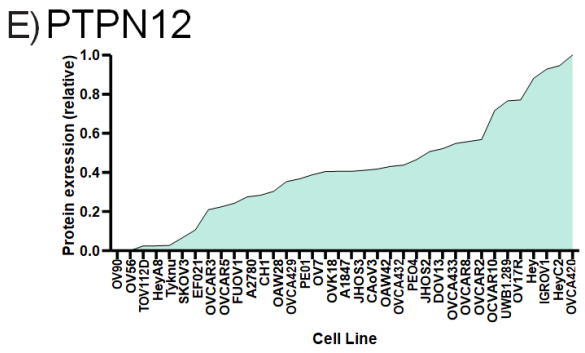

Figure 2E: Relative, normalised expression level of PTPN12 in ovarian cancer cell lines ranked by ascending expression. Seven cell lines had very low expression of PTPN12.

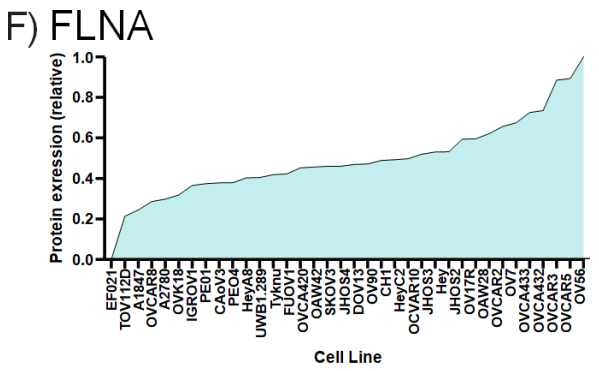

Figure 2F: Relative, normalised expression level of FLNA in Ovarian cancer cell lines ranked by ascending expression. One cell line, EF021, did not express FLNA.

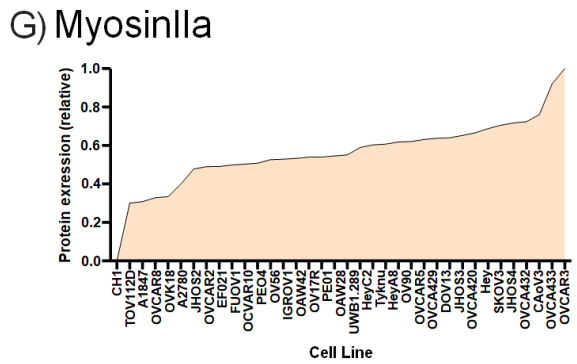

Figure 2G: Relative, normalised expression level of Myosin IIa in Ovarian cancer cell lines ranked by ascending expression. One cell line, CH1, had no expression of Myosin IIa.

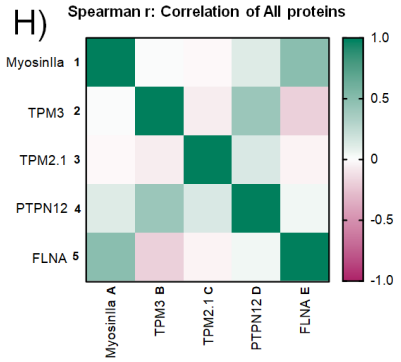

Figure 2H: Correlation between the expressions of all proteins was tested by Spearman rank correlation. PTPN12 and TPM3 were postively correlated, with a R2 of 0.414. MyosinIIa and FLNA were positively correlated with and R2 of 0.493.

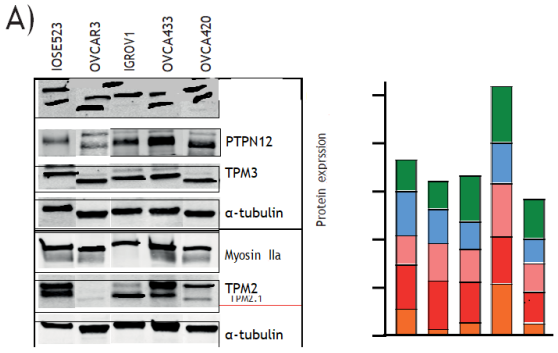

Figure 3A: Western blots of selected cell lines showing Filamin A, PTPN12, TPM3, and a-tubulin.

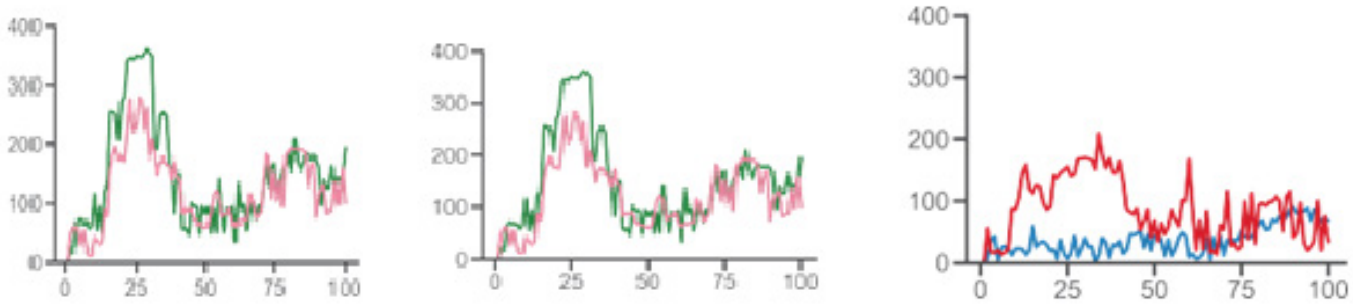

Figure 3B: Close up image of deflections of four pillars, taken from still from BJ cells. **Note:** (—) Pillar 1; (—) Pillar 2; (—) Pillar 3; (—) Pillar 4.

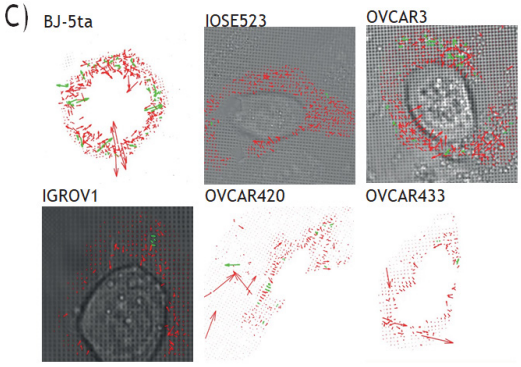

Figure 3C: Cells were plated on 0.8 um micropilars and imaged at 1 frame per second for 30 minutes.

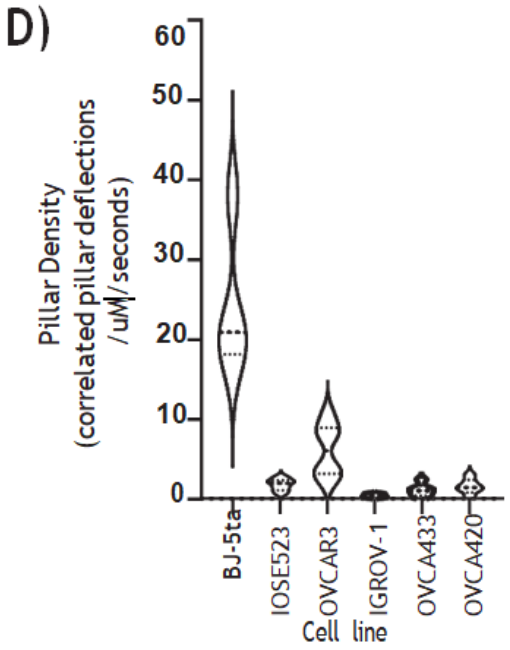

Figure 3D: Significant difference between BJ cells and all other cell lines, determined by one way ANOVA with Tukey correction.

The movies from this imaging were processed by removing drift using the ImageJ plugin stackreg with translation, detecting and tracking pillars with the ImageJ plugin Pilartracker and calculating the correlated pillar deflections using a custom script for Matlab. Based upon the unbiased computer analysis, the HFF (BJ-5ta) cells had a density of rigidity sensing 24.27 events per second per µm2 (N=4). In contrast, all the ovarian cells lines had a significantly lower number of contractile events. IOSE523 cells had a mean of 1.8 (n=7) contractile pairs per second per µm2, OVCAR3 cells had a mean of 6.13 (n=6), IGROV1 cells had a mean of 0.49 (n=5), OVCA433 cells had a mean of 1.18 (n=5) and OVCA420 (n=5) cells had a mean of 1.57 contractile units per second per µm2, where in is the number of individual cells. Thus, all of the tumor cells, and the transformed ovarian epithelial cell line lacked rigidity sensing contractions, which further supported the hypothesis that tumor formation involved the loss of rigidity sensing.

Previously it has been demonstrated that one marker of cells capacity to detect changes in substrate stiffness is reflected in how their actin is aligned [63-66]. Non-transformed cells on soft surfaces have a low alignment of actin and do not form polarised stress fibres, while on rigid substrates actin fibers align in a coordinated direction and the cell polarises. Using this criterion, we tested the alignment of actin filaments by imaging f-actin using a phalloidin stain and calculating the nematic order parameter of each cell on two PDMS substrates of different stiffness, 2MPa and 5kPa [67]. To quantify actin ordering, images were cropped to single cell images and nematic order parameter was measured using a custom Matlab script [68]. This gave a single numerical value for the alignment score of the actin filaments between 1 and 0, 1 being all fibres in the same direction and 0 being no fibres in the same direction. In non-transformed fibroblasts, a significant difference in actin alignment was observed between 5 kPa and 2 MPa. On stiffer substrates, fibroblasts had a more ordered actin structure with higher polarization but on softer substrates, they had a more disordered actin [69] (Figure 4A), and it is significantly higher nematic order parameter was observed in the negative control BJ-3ta HFF cells plated on 2 MPa compared to 5 kPa. In contrast, none of the ovarian cell lines demonstrated a significant difference in the nematic order of actin between soft and rigid substrates (Figures 4B and 4C), including the ovarian epithelial line IOSE523. This ovarian epithelial line, although not cancerous in origin, is SV-40 transformed and has lost the capacity to sense substrate stiffness [70].

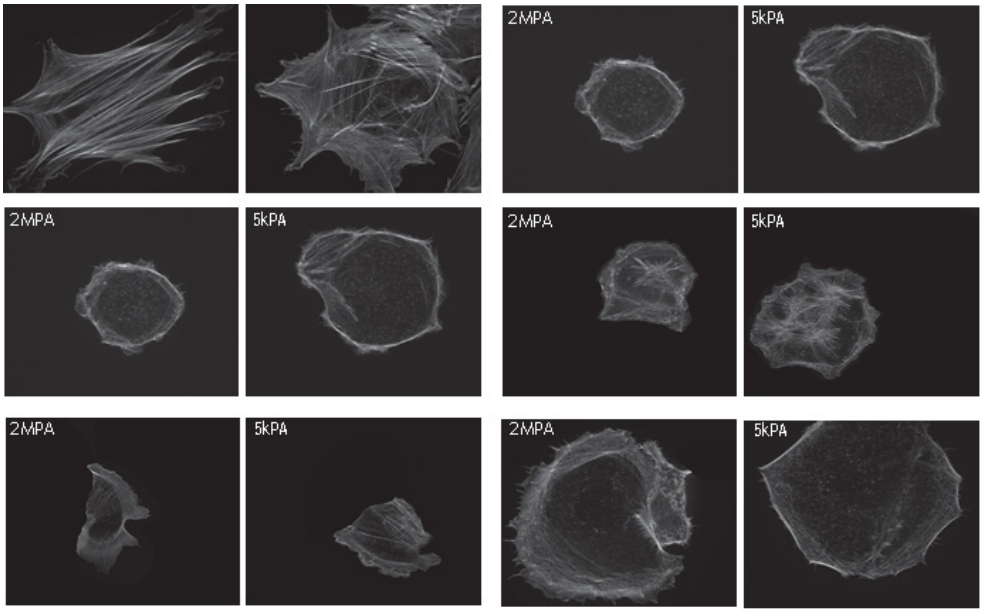

Figure 4A: Images of Phalloidin staining for f-actin in six cell lines on PDMS surfaces of 2MPa and 5kPa stiffness.

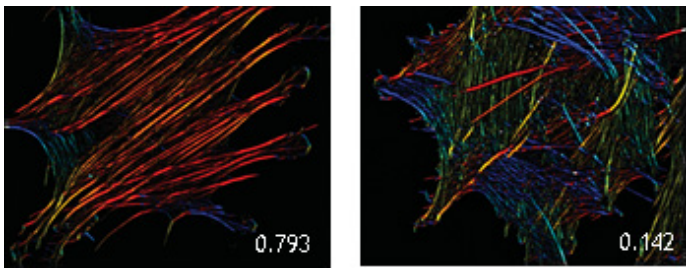

Figure 4B: Example images of actin alignment quantification in HFF (BJ-5ta) cells on 2 MPa (top) and 5 kPa (bottom) with the nematic order perameters of 0.793 and 0.142 respectively. Images are output from the custom matlab script and are colour coded by actin fibre angle.

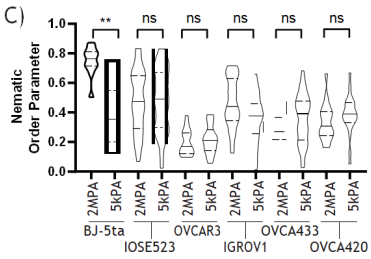

Figure 4C: Quantification of the nematic order perameter in each cell line on both surfaces. There was a significantly higher nematic order peramter on 2 MPa PDMS in HFF cells vs. HFF cells on 5 kPa PDMS. No other cell line had significant differences in nematic order peramter between 2 MPa and 5 kPa PDMS.

Through these two methods, measuring the correlated pillar deflections in spreading cells and the nematic order perameter of actin after cell spreading, we show that the remaining cell lines that retained all the proteins assayed phenotypically were unable to sense a change in substrate stiffness in actin alignment, nor were they able to pinch micro pillars during the spreading phase of attachment. These cell lines we propose have lost rigidity sensing by currently unknown.

DISCUSSION

In this study, all of the ovarian tumor lines tested lack the ability to sense rigidity. There are many differences in the levels of expression of mechanosensory proteins but about 75% of the lines are missing one of the proteins known to be needed for rigidity sensing. Half of the cell lines lack TPM2.1, 20% are depleted of PTPN12 and there are occasional losses of FilaminA or Myosin IIA; but in several cases the basis of the loss in rigidity sensing is unknown. However, the fact that all lines appear to lack rigidity sensing is consistent with the hypothesis that transformation is necessary for tumor formation and transformation results from the loss of rigidity sensing.

Because the rigidity sensor is a complex modular machine with many different components, it is expected that the loss of any one of many different components could block rigidity sensing. Studies

have found that rigidity sensing is lost and transformed growth is gained upon the depletion of at least eight different proteins [71]. Like any complex process that involves many proteins, there are many possible ways to block function. This is consistent with the general diversity of mutations that give rise to cancer. What is not considered here are the many developmental changes that are involved in large tumor growth and metastasis. Progression in cancer is enabled by transformation, since with some growth; cells can evolve or develop the best systems for growth in their microenvironment. Thus, although the loss of function in any one of a large group of proteins can cause transformation, an even larger number of alterations are needed for tumor growth or metastasis.

TPM2.1 has already been shown to be down regulated in breast, colorectal and urothelial bladder cancer [72]. Here we show that TMP2.1 is commonly down regulated or lost in ovarian cancer cells, further providing evidence for TMP2.1 as a tumour suppressor. TPM3, however is most often overexpressed, and is rarely lost throughout this panel of ovarian cancer cell lines, providing evidence of a potential role as an oncogene. From the many different phenotypes of cancer cells even with the loss of rigidity sensing proteins, the common mechanosensing defects in cancer cells are not evident. In particular, the epithelial to mesenchyme transition may increase cell motility and the risk of metastasis or severe disease, however, the loss of rigidity sensing or transformation appears to be a common feature of nearly all tumor cells irrespective of EMT.

The transformed phenotype involves more than the ability to grow on soft agar. Studies of tumor cells, indicate that in general they are softer (more easily deformed), they generate higher traction forces and they are damaged by mechanical perturbations. This is likely only a partial list of the complex functions that are altered with transformation since the mRNA levels of several hundred proteins are altered by the simple expression of TPM2.1 in tumor cells or the depletion of TPM2.1 in fibroblasts. Transformation appears to be a state change that involves a concerted alteration of a characteristic set of functions.

Becoming insensitive to substrate stiffness has several advantages for a cancer cell, firstly they are able to ignore cues in their environment which normally signal them to slow down proliferation, or activate them for apoptosis. It has previously been shown that, in non-cancer cells, plating on soft surfaces initiates a signalling cascade for caspase mediated apoptosis [73] in losing mechanosensitive proteins this signal is ablated or at least weakened meaning that cancer cells can avoid death by avoiding this signalling pathway. Secondly, as cancer cells metastasize, it is conceivable that they will encounter various substrates from collagen to vascular systems and others [74,75], and being able to adapt to changing mechanical environments would make them more likely to survive to produce metastatic tumours.

The general changes in functions that are common to transform cells and most if not all tumor cells are potentially very important in indicating ways to inhibit growth of many different tumor cells. In this regard, the mechanical sensitivity of transformed cells is potentially interesting [76-79]. Not only has the fluid shear of tumor cells but also mechanical stretching caused apoptosis. Further, there are indications that mechanical perturbation of tumors in vivo will also inhibit their growth. Other aspects of the transformed state have not been systematically analysed to determine if other treatments would inhibit growth of tumor cells but not their normal cell neighbors [80].

CONCLUSION

In summary, these findings show that the transformed state is a common characteristic of a diverse set of tumor cells that show many different behaviors and that the transformed state correlates with the loss of rigidity sensing. This supports the hypothesis that transformation is necessary but not sufficient for tumor growth. Further, the characteristic changes in functions upon transformation may be exploited to aid in the selective inhibition of transformed cell growth.

REFERENCES

1. Bedolla RG, Wang Y, Asuncion A, Chamie K, Siddiqui S, Mudryj MM, et al. Nuclear versus cytoplasmic localization of filamin A in prostate cancer: immunohistochemical correlation with metastases. Clin Cancer Res. 2009;15(3):788-796.
2. Berg JS, Powell BC, Cheney RE. A millennial myosin census. Mol Biol Cell. 2001;12(4):780-794.
3. Berrueta L, Bergholz J, Munoz D, Muskaj I, Badger GJ, Shukla A, et al. Stretching reduces tumor growth in a mouse breast cancer model. Sci Rep. 2018;8(1):1-7.
4. Betof AS, Lascola CD, Weitzel D, Landon C, Scarbrough PM, Devi GR, et al. Modulation of murine breast tumor vascularity, hypoxia, and chemotherapeutic response by exercise. J Natl Cancer Inst. 2015;107(5).
5. Bosch R, Dieguez-Gonzalez R, Cespedes MV, Parreno M, Pavon MA, Granena A, et al. A novel inhibitor of focal adhesion signaling induces caspase-independent cell death in diffuse large B-cell lymphoma. Blood J Am Soc Hematol. 2011;118(16):4411-4420.
6. Byron A, Morgan MR, Humphries MJ. Adhesion signalling complexes. Curr Biol. 2010;20(24):R1063-R1067.
7. Chang CW, Chen CR, Huang CY, Shu WY, Chiang CS, Hong JH, et al. Comparative transcriptome profiling of an SV40-transformed human fibroblast (MRC5CVI) and its untransformed counterpart (MRC-5) in response to UVB irradiation. PloS one. 2013;8(9):e73311.
8. Chen H, Chandrasekar S, Sheetz MP, Stossel TP, Nakamura F, Yan J. Mechanical perturbation of filamin A immunoglobulin repeats 20-21 reveals potential non-equilibrium mechanochemical partner binding function. Sci Rep. 2013;3(1):1-6.
9. Chiang SP, Cabrera RM, Segall JE. Tumor cell intravasation. Am J Physiol-Cell Physiol. 2016;311(1):C1-C4.
10. Coughlin MF, Bielenberg DR, Lenormand G, Marinkovic M, Waghorne CG, Zetter BR, et al. Cytoskeletal stiffness, friction, and fluidity of cancer cell lines with different metastatic potential. Clin Exp Metast. 2013;30(3):237-250.
11. Coussens LM, Werb Z. Inflammation and cancer. Nature. 2002;420(6917):860-867.
12. Cross SE. Jin YS, Rao J, Gimzewski JK. Nanomechanical analysis of cells from cancer patients. Nat Nanotechnol. 2007;2:780-783.
13. Cui J, Cai Y, Hu Y, Huang Z, Luo Y, Kaz AM, et al. Epigenetic silencing of TPM2 contributes to colorectal cancer progression upon RhoA activation. Tumor Biol. 2016;37(9):12477-12483.
14. Dube S, Chionuma H, Matoq A, Alshiekh-Nasany R, Abbott L, Poiesz BJ, et al. Expression of various sarcomeric tropomyosin isoforms in equine striated muscles. Open Vet J. 2017;7(2):180-191.
15. Feitelson MA, Arzumanyan A, Kulathinal RJ, Blain SW, Holcombe RF, Mahajna J, et al. Sustained proliferation in cancer: Mechanisms and novel therapeutic targets. Semin Cancer Biol. 2015;35:S25-S54.
16. Feng YH, Tsao CJ. Emerging role of microRNA-21 in cancer. Biomed Rep. 2016;5(4):395-402.

17. Gunning PW, Hardeman EC, Lappalainen P, Mulvihill DP. Tropomyosin-master regulator of actin filament function in the cytoskeleton. J Cell Sci. 2015;128(16):2965-2974.

18. Gupta M, Doss BL, Kocgozlu L, Pan M, Mege RM, Callan-Jones A, et al. Cell shape and substrate stiffness drive actin-based cell polarity. Phys Rev E. 2019;99(1):012412.

19. Gupta M, Doss B, Lim CT, Voituriez R, Ladoux B. Single cell rigidity sensing: A complex relationship between focal adhesion dynamics and large-scale actin cytoskeleton remodeling. Cell Adh Migr. 2016;10(5):554-567.

20. Gupta M, Sarangi BR, Deschamps J, Nematbakhsh Y, Callan-Jones A, Margadant F, et al. Adaptive rheology and ordering of cell cytoskeleton govern matrix rigidity sensing. Nat commun. 2015;6(1):1-9.

21. Hamburger A, Salmon SE. Primary bioassay of human myeloma stem cells. J Clin Investig. 1977;60(4):846-854.

22. Harari PM. Epidermal growth factor receptor inhibition strategies in oncology. Endocr-Relat Cancer. 2004;11(4):689-708.

23. Hart J. Inflammation 2: Its role in the healing of chronic wounds. J Wound Care. 2002;11(7):245-249.

24. Holman EC, Campbell LJ, Hines J, Crews CM. Microarray analysis of microRNA expression during axolotl limb regeneration. PloS one. 2012;7.

25. Hu X, Margadant FM, Yao M, Sheetz MP. Molecular stretching modulates mechanosensing pathways. Protein Sci. 2017;26(7):1337-1351.

26. Huang RY, Wong MK, Tan TZ, Kuay KT, Ng AH, Chung VY, et al. An EMT spectrum defines an anoikis-resistant and spheroidogenic intermediate mesenchymal state that is sensitive to e-cadherin restoration by a src-kinase inhibitor, saracatinib (AZD0530). Cell Death Dis. 2013;4(11):e915.

27. Humayun-Zakaria N, Arnold R, Goel A, Ward D, Savill S, Bryan RT. Tropomyosins: Potential biomarkers for urothelial bladder cancer. International J Mol Sci. 2019;20(5):1102.

28. Il'yasova D, Colbert LH, Harris TB, Newman AB, Bauer DC, Satterfield S, et al. Circulating levels of inflammatory markers and cancer risk in the health aging and body composition cohort. Cancer Epidemiol Biomark Prev. 2005;14(10):2413-2418.

29. Iwanicki MP, Davidowitz RA, Ng MR, Besser A, Muranen T, Merritt M, et al. Ovarian cancer spheroids use myosin-generated force to clear the mesothelium contractile forces generated by ovarian cancer spheroids promote mesothelial clearance. Cancer Discovery. 2011;1(2):144-157.

30. Kapoor A, Barai A, Thakur B, Das A, Patwardhan SR, Monteiro M, et al. Soft drug-resistant ovarian cancer cells migrate via two distinct mechanisms utilizing myosin II-based contractility. Biochim Biophys Acta Mol Cell Res BBA. 2018;1865(2):392-405.

31. Kiema T, Lad Y, Jiang P, Oxley CL, Baldassarre M, Wegener KL, et al. The molecular basis of filamin binding to integrins and competition with talin. Mol Cell. 2006;21(3):337-347.

32. Krendel M, Mooseker MS. Myosins: Tails (and heads) of functional diversity. Physiol. 2005;20(4):239-251.

33. Landen NX, Li D, Stahle M. Transition from inflammation to proliferation: A critical step during wound healing. Cell Mol Life Sci. 2016;73(20):3861-3885.

34. Li YR, Yang WX. Myosins as fundamental components during tumorigenesis: Diverse and indispensable. Oncotarget. 2016;7(29):46785-46812.

35. Li Z, Persson H, Adolfsson K, Abariute L, Borgstrom MT, Hessman D, et al. Cellular traction forces: A useful parameter in cancer research. Nanoscale. 2017;9(48):19039-19044.

36. Lin HH, Lin HK, Lin IH, Chiou YW, Chen HW, Liu CY, et al. Mechanical phenotype of cancer cells: Cell softening and loss of stiffness sensing. Oncotarget. 2015;6(25):20946-20958.

37. Malfatti E, Neto OA, Fardeau M, Laporte J, Romero N. Novel histopathological phenotypes associated with TPM2 and TPM3-related congenital myopathies. Neuromuscul Disord. 2015;25:S288.

38. Marquez RT, Wendlandt E, Galle CS, Keck K, McCaffrey AP. MicroRNA-21 is upregulated during the proliferative phase of liver regeneration, targets Pellino-1, and inhibits NF-κB signaling. Am J Physiol Gastrointest Liver Physiol. 2010;298(4):G535-G541.

39. Maslikowski BM, Wang L, Wu Y, Fielding B, Bedard PA. JunD/AP-1 antagonizes the induction of DAPK1 to promote the survival of v-Src-transformed cells. J Virol. 2016;91(1):e01925-e02016.

40. McIlwain DR, Berger T, Mak TW. Caspase functions in cell death and disease. Cold Spring Harb Perspect Biol. 2013;5(4):a008656.

41. Meacci G, Wolfenson H, Liu S, Stachowiak MR, Iskratsch T, Mathur A, et al. α-Actinin links extracellular matrix rigidity-sensing contractile units with periodic cell-edge retractions. Mol Biol Cell. 2016;27(22):3471-3479.

42. Melli L, Billington N, Sun SA, Bird JE, Nagy A, Friedman TB, et al. Bipolar filaments of human nonmuscle myosin 2-A and 2-B have distinct motile and mechanical properties. Elife. 2018;7:e32871.

43. Michels N, Van Aart C, Morisse J, Huybrechts I. Chronic inflammation toward cancer incidence: An epidemiological systematic review. Crit Rev Oncol Hematol. 2021;157:103177.

44. Morgan-Parkes JH. Metastases: Mechanisms, pathways, and cascades. Am J Roentgenol. 1995;164(5):1075-1082.

45. Nagano T, Tachihara M, Nishimura Y. Mechanism of resistance to epidermal growth factor receptor-tyrosine kinase inhibitors and a potential treatment strategy. Cell. 2018;7(11):212.

46. Nakamura F, Heikkinen O, Pentikainen OT, Osborn TM, Kasza KE, Weitz DA, et al. Molecular basis of filamin A-FilGAP interaction and its impairment in congenital disorders associated with filamin A mutations. PLoS One. 2009;4(3):e4928.

47. Nakamura F, Osborn TM, Hartemink CA, Hartwig JH, Stossel TP. Structural basis of filamin A functions. J Cell Biol. 2007;179(5):1011-1025.

48. Nakamura F, Song M, Hartwig JH, Stossel TP. Documentation and localization of force-mediated filamin A domain perturbations in moving cells. Nat Commun. 2014;5(1):1-11.

49. Nallapalli RK, Ibrahim MX, Zhou AX, Bandaru S, Sunkara SN, Redfors B, et al. Targeting filamin A reduces K-RAS-induced lung adenocarcinomas and endothelial response to tumor growth in mice. Mol Cancer. 2012;11(1):1-11.

50. Nomachi A, Nishita M, Inaba D, Enomoto M, Hamasaki M, Minami Y. Receptor tyrosine kinase Ror2 mediates Wnt5a-induced polarized cell migration by activating c-Jun N-terminal kinase via actin-binding protein filamin A. J Biol Chem. 2008;283(41):27973-27981.

51. Ouderkirk JL, Krendel M. Non-muscle myosins in tumor progression, cancer cell invasion, and metastasis. Cytoskeleton. 2014;71(8):447-463.

52. Pecci A, Ma X, Savoia A, Adelstein RS. MYH9: Structure, functions and role of non-muscle myosin IIA in human disease. Gene. 2018;664:152-167.

53. Peschetola V, Laurent VM, Duperray A, Michel R, Ambrosi D, Preziosi L, et al. Time-dependent traction force microscopy for cancer cells as a measure of invasiveness. Cytoskeleton. 2013;70(4):201-214.

54. Prager-Khoutorsky M, Lichtenstein A, Krishnan R, Rajendran K, Mayo A, Kam Z, et al. Fibroblast polarization is a matrix-rigidity-dependent process controlled by focal adhesion mechanosensing. Nat Cell Biol. 2011;13(12):1457-1465.

55. Qin R, Wolfenson H, Saxena M, Sheetz MP. Tumor suppressor DAPK1 catalyzes adhesion assembly on rigid but anoikis on soft matrices. Biorxiv. 2018:320739.

56. Sarangi BR, Gupta M, Doss BL, Tissot N, Lam F, Mege RM, et al. Coordination between intra-and extracellular forces regulates focal adhesion dynamics. Nano Let. 2017;17(1):399-406.

57. Savant SS, Sriramkumar S, O'Hagan HM. The role of inflammation and inflammatory mediators in the development, progression, metastasis, and chemoresistance of epithelial ovarian cancer. Cancer. 2018;10(8):251.

58. Savoy RM, Ghosh PM. The dual role of filamin A in cancer: Can't live with (too much of) it, can't live without it. Endocr-Relat Cancer. 2013;20(6):R341-R356.

59. Saxena M, Liu S, Yang B, Hajal C, Changede R, Hu J, et al. EGFR and HER2 activate rigidity sensing only on rigid matrices. Nat Mater. 2017;16(7):775-781.

60. Sheetz M. A tale of two states: Normal and transformed, with and without rigidity sensing. Annu Rev Cell Dev Biol. 2019;35:169-190.

61. Stefen H, Suchowerska AK, Chen BJ, Brettle M, Kuschelewski J, Gunning PW, et al. Tropomyosin isoforms have specific effects on the transcriptome of undifferentiated and differentiated B35 neuroblastoma cells. FEBS Open Bio. 2018;8(4):570-583.

62. Stoletov K, Kato H, Zardouzian E, Kelber J, Yang J, Shattil S, et al. Visualizing extravasation dynamics of metastatic tumor cells. J Cell Sci. 2010;123(13):2332-2341.

63. Sun T, Aceto N, Meerbrey KL, Kessler JD, Zhou C, Migliaccio I, et al. Activation of multiple proto-oncogenic tyrosine kinases in breast cancer via loss of the PTPN12 phosphatase. Cell. 2011;144(5):703-718.

64. Sundararajan V, Tan M, Tan TZ, Ye J, Thiery JP, Huang RY. SNAI1 recruits HDAC1 to suppress SNAI2 transcription during epithelial to mesenchymal transition. Sci Rep. 2019;9(1):1-9.

65. Swaminathan V, Mythreye K, O'Brien ET, Berchuck A, Blobe GC, Superfine R. Mechanical stiffness grades metastatic potential in patient tumor cells and in cancer cell lines: Mechanical stiffness of cells dictates cancer cell invasion. Cancer Res. 2011;71(15):5075-5080.

66. Takao S, Taya M, Chiew C. Mechanical stress-induced cell death in breast cancer cells. Biol Open. 2019;8(8):bio043133.

67. Tan TZ, Miow QH, Huang RY, Wong MK, Ye J, Lau JA, et al. Functional genomics identifies five distinct molecular subtypes with clinical relevance and pathways for growth control in epithelial ovarian cancer. EMBO Mol Med. 2013;5(7):1051-1066.

68. Tan TZ, Miow QH, Miki Y, Noda T, Mori S, Huang RY, et al. Epithelial-mesenchymal transition spectrum quantification and its efficacy in deciphering survival and drug responses of cancer patients. EMBO Mol Med. 2014;6(10):1279-1293.

69. Tan TZ, Yang H, Ye J, Low J, Choolani M, Tan DS, et al. CSIOVDB: A microarray gene expression database of epithelial ovarian cancer subtype. Oncotarget. 2015;6(41):43843-43852.

70. Tijore A, Yao M, Wang YH, Nematbakhsh Y, Hariharan A, Lim CT, et al. Mechanical stretch kills transformed cancer cells. Biorxiv. 2018:491746.

71. Todoric J, Antonucci L, Karin M. Targeting inflammation in cancer prevention and therapy. Cancer Prev Res. 2016;9(12):895-905.

72. Vicente-Manzanares M, Ma X, Adelstein RS, Horwitz AR. Non-muscle myosin II takes centre stage in cell adhesion and migration. Nat Rev Mol Cell Biol. 2009;10(11):778-790.

73. Villa-Moruzzi E. Tyrosine phosphatases in the HER2-directed motility of ovarian cancer cells: Involvement of PTPN12, ERK5 and FAK. Anal Cell Pathol. 2011;34(3):101-112.

74. Wang T, Feng Y, Sun H, Zhang L, Hao L, Shi C, et al. miR-21 regulates skin wound healing by targeting multiple aspects of the healing process. Am J Pathol. 2012;181(6):1911-1920.

75. Wolfenson H, Meacci G, Liu S, Stachowiak MR, Iskratsch T, Ghassemi S, et al. Tropomyosin controls sarcomere-like contractions for rigidity sensing and suppressing growth on soft matrices. Nat Cell Biol. 2016;18(1):33-42.

76. Wu Y, Song Y, Xiong Y, Wang X, Xu K, Han B, et al. MicroRNA-21 (Mir-21) promotes cell growth and invasion by repressing tumor suppressor PTEN in colorectal cancer. Cell Physiol Biochem. 2017;43(3):945-958.

77. Yang B, Wolfenson H, Chung VY, Nakazawa N, Liu S, Hu J, et al. Stopping transformed cancer cell growth by rigidity sensing. Nat Mater. 2020;19(2):239-250.

78. Yoshida H, Cheng W, Hung J, Montell D, Geisbrecht E, Rosen D, et al. Lessons from border cell migration in the Drosophila ovary: A role for myosin VI in dissemination of human ovarian cancer. Proc Natl Acad Sci. 2004;101(21):8144-8149.

79. Yue J, Huhn S, Shen Z. Complex roles of filamin-A mediated cytoskeleton network in cancer progression. Cell Biosci. 2013;3(1):1-2.

80. Zhang H, Wang Y, Lv Q, Gao J, Hu L, He Z. MicroRNA-21 overexpression promotes the neuroprotective efficacy of mesenchymal stem cells for treatment of intracerebral hemorrhage. Front Neurol. 2018;9:931.